nature publishing group

Establishment of a method for evaluating endothelial cell injury by TNF-α *in vitro* for clarifying the pathophysiology of virus-associated acute encephalopathy

Kyohei Miyazaki[1], Koichi Hashimoto[1], Masatoki Sato[1], Masahiro Watanabe[1], Naoki Tomikawa[2], Shuto Kanno[1], Yukihiko Kawasaki[1], Nobuo Momoi[1] and Mitsuaki Hosoya[1]

BACKGROUND: Virus-associated acute encephalopathy (VAE) is a severe central nervous system complication caused by common viral infections in children. The pathophysiology of VAE is thought to be endothelial injury. This study was designed to establish an *in vitro* VAE model for evaluating endothelial injury caused by the proinflammatory cytokine TNF-α.

METHODS: Transwell-grown human umbilical vein endothelial cells (HUVECs) monolayers were incubated with serially diluted TNF-α. Transendothelial electrical resistance (TER) was measured using impedance spectroscopy. Permeability changes of HUVECs after TNF-α treatment were determined by fluorescein isothiocyanate (FITC)-conjugated dextran. Moreover, TNF-α-induced morphological changes in claudin-5 and apoptosis were observed by immunofluorescent staining.

RESULTS: The decrease in TER, time of TER recovery to baseline, and increase in permeability were all dependent on TNF-α concentration. Immunofluorescent staining showed that claudin-5 was delocalized after TNF-α treatment in a dose-dependent manner. In addition, some apoptotic cells were observed at high TNF-α concentrations.

CONCLUSION: TER measurement combined with a permeability assay could be useful for evaluating vascular endothelial cell permeability in an *in vitro* model. These evaluation methods will contribute to both the development of specific treatments focusing on vascular permeability, and the search for a novel therapeutic strategy in VAE treatment.

Virus-associated acute encephalopathy (VAE) is a severe complication in children caused by common viral infections such as influenza, human herpes virus-6, rotavirus, and other viruses. Clinical characteristics of VAE are the acute onset of neurological manifestations, such as impaired consciousness and convulsions following viral febrile infection without pleocytosis in cerebrospinal fluid (1,2). VAE is one of the major causes of neurological morbidity and mortality in children without underlying diseases. Proinflammatory cytokine levels in serum, such as tumor necrosis factor-alpha (TNF-α), interleukin-1β (IL-1β), and interleukin-6 (IL-6), were abnormally higher in the acute stage of severe VAE cases than those in the controls and febrile convulsion cases (3–5). Pathological studies of the brain at necropsy demonstrated that severe brain edema and plasma extravasation occurred in severe VAE cases (1,6). This indicates that blood–brain barrier disruption had occurred. To date, the pathophysiology of VAE has been classified into three major categories based on clinical, laboratory, imaging, and pathological findings of VAE: cytokine storm type; excitotoxicity type; and metabolic error type (1). The mortality rate of cytokine storm type VAE cases is higher than that of all VAE cases including cytokine storm type; about 30% and less than 10%, respectively (1,7,8).

It has been hypothesized that the pathophysiology of cytokine storm type is attributable to the extreme production of proinflammatory cytokines that induce vascular endothelial cell dysfunction, resulting in deterioration of vascular permeability. This permeability is restricted by tight junctions, which exist in endothelial and epithelial cells (9). Various cytokines, including TNF-α, affect the regulation of vascular permeability by directly modifying tight junction composition and structure through signaling pathways independent of cell death (10).

Tight junctions are the apical-most constituent of the junctional complex in endothelial cells, and appear as a series of very close membrane appositions between adjacent cells. These contact sites principally correspond to a continuous network of intramembranous particle fibrils (tight junction strands). They contribute to signal transduction, and act as a barrier to the paracellular transport of ions, solutes, and water, thereby distinguishing the apical and basal plasma membranes (11). Claudins are constituents of a tight junction complex, and are expressed in epithelial and endothelial cells in a variety of tissues. There are currently 27 known members of the claudin family including claudin-5, which is specifically expressed and plays a crucial role in regulating vascular permeability (12–14).

Transendothelial electrical resistance (TER) measurement and permeability assay are two useful parameters in the

[1]Department of Pediatrics, Fukushima Medical University, Fukushima, Japan; [2]Department of Basic Pathology, Fukushima Medical University, Fukushima, Japan.
Correspondence: Kyohei Miyazaki (kyon0421@fmu.ac.jp)

Received 17 July 2016; accepted 15 December 2016; advance online publication 5 April 2017. doi:10.1038/pr.2017.28

determination of vascular permeability in an *in vitro* model. TER measurement quantifies barrier properties by measuring electrical resistance between the upper and lower surfaces of monolayer-cultured endothelial cells. A permeability assay measures the fluorescence intensity of fluorescein isothiocyanate (FITC)-conjugated dextran permeating through monolayer-cultured cells. These tools can analyze the hyper- and hypopermeability states of endothelial cells electrophysiologically and functionally (15).

Although the pathogens, pathophysiology, and classification of VAE are being clarified, the precise mechanism of endothelial injury caused by cytokines in VAE has not yet been fully explained. Furthermore, VAE *in vivo* or *in vitro* model that describes the pathophysiology of VAE has not been established yet. This study was designed to establish a method for evaluating endothelial injury caused by proinflammatory cytokines *in vitro* with implicated pathophysiology of VAE. To clarify the dynamics of vascular dysfunction caused by TNF-α, this study was performed as follows: electrophysiological measurement of TER, functional permeability assay, and pathological immunofluorescent staining for claudin-5. In addition, to investigate the involvement of apoptosis, cleaved caspase-3 staining and terminal deoxynucleotidyl transferase (TdT)-mediated deoxyuridine triphosphate (dUTP) nick end labeling (TUNEL) staining were performed.

METHODS

Materials

Recombinant human TNF-α protein was purchased from R&D System (Minneapolis, MN). FITC-conjugated dextran (average mol wt 70,000) and non-FITC-conjugated dextran (average mol wt 64,000–76,000) were purchased from SIGMA–ALDRICH (St. Louis, MO).

Human Umbilical Vein Endothelial Cells (HUVECs)

Human umbilical vein endothelial cells (HUVECs) were isolated from umbilical cords and cultured using a modified procedure as previously described (16,17). Primary HUVECs, which were isolated using 0.25% trypsin/14 mM EDTA (Denka Seiken, Tokyo, Japan), were cultured on Corning BioCoat Gelatin Rectangular Canted Neck Culture Flasks w/Vented Cap (CORNING, Rochester, NY) in MCDB131 medium (Cosmo Bio, Tokyo, Japan) containing 10% fetal bovine serum (FBS; Equitech-Bio, Kerrville, TX), 4 ng/ml aFGF (WAKO Pure Chemical Industries, Osaka, Japan), 10 ng/ml EGF (WAKO Pure Chemical Industries), 50 μg/ml heparin (Gibco Life Technologies, Grand Island, NY), 1 μg/ml hydrocortisone (WAKO Pure Chemical Industries), and 50 μg/ml Gentamicin (Nacalai Tesque, Kyoto, Japan) at 37 °C under humidified 5% CO_2. After the HUVECs were confluent, they were trypsinized and stored at a temperature of −80 °C until use. These HUVECs were cultured on Transwell (cat. no. 3470; pore size 0.4μm; CORNING) inserts using EBM-2 medium with an EGM-2 bullet kit containing 2% FBS, antibiotics, and a mixture of growth factors according to the supplier's instructions (LONZA JAPAN, Tokyo, Japan) at 37 °C under humidified 5% CO_2. The medium was replaced every 2 d until confluent. The HUVECs were seeded at 1×10^5 cells/cm^2 and cultured on type I collagen-coated 24-well Transwell inserts. Type I collagen, Cellmatrix was purchased from Nitta Gelatin, Osaka, Japan. Isolated HUVECs were confirmed by immunofluorescence staining using anti mouse CD31 monoclonal antibody (Ab) (DAKO Japan, Kyoto, Japan) as an endothelial cell marker (data not shown).

The ethics committee of Fukushima Medical University approved this study. Written informed consent was obtained from all participants who donated umbilical cords.

Transendothelial Electrical Resistance (TER) Measurement

HUVECs were cultured on type-I collagen-coated membranes on 24-well Transwell inserts. These inserts were set in the cellZscope (nanoAnalytics GmbH, Münster, Germany) and TER measurement was started. After TER became stable, serially diluted TNF-α was added to the medium in both the upper and lower compartments of the wells at final concentrations of 0 pg/ml (control), 100 pg/ml, 500 pg/ml, and 2,500 pg/ml. The TER level was measured over time automatically after treatment of the HUVECs monolayer at each TNF-α concentration. The TER values of the samples were corrected by the mean TER level of no-cell-cultured inserts by the cellZscope software. The TER levels correlate with the strength of the tight junctions between adjacent cells; high and low TER values indicate low and high tight junction permeability, respectively (18).

Permeability Assay

HUVECs were cultured on 24-well Transwell inserts as described above. At specific time points (8, 12, 30, 57, 82, and 96 h) after treatment with TNF-α, FITC-conjugated dextran and non-FITC-conjugated dextran were administered to the upper and lower compartments of the inserts, respectively, to maintain the same osmotic pressure (19). The upper and lower compartments represent the intravascular and extravascular spaces, respectively; so, this model represents solute permeation from the intravascular to extravascular space. One hour after adding dextran, the fluorescence intensity of the medium in the lower compartments was measured by the fluorescent micro plate reader Fluoroskan (Thermo Fisher Scientific, San Jose, CA), at an excitation of 485 nm and emission of 538 nm. The FITC-conjugated dextran concentration was calculated with a standard curve.

Immunofluorescent Staining

Transwell-grown HUVECs monolayers were incubated with serially diluted TNF-α, and immunofluorescent staining was performed using wells that were used in a previously described permeability assay (20). Briefly, cells were fixed in ice-cold acetone for 15 min at −20 °C, followed by permeabilization with ice-cold methanol for 20 min at −20 °C. After washing with phosphate-buffered saline (PBS), the cells were blocked in PBS with 3% bovine serum albumin (BSA) and 0.3% Triton-X 100 for 1 h at room temperature, then incubated with anti claudin-5 mouse monoclonal Ab (1:200, Invitrogen, Carlsbad, CA) for tight junction staining, anti cleaved caspase-3 rabbit polyclonal Ab (Cell Signaling technology, Beverly, MA) for apoptosis detection, and anti mouse CD31 monoclonal Ab for confirmation of HUVECs as the primary Ab at 4 °C overnight. Subsequently, the cells were incubated with donkey Cy3 AffiniPure F(ab')2 Frag Donkey Anti Mouse IgG (Jackson Immuno Research Laboratories, West Grove, PA) and Alexa Fluor 488 Goat Anti-Rabbit IgG (Molecular Probes, Eugene, OR) as the secondary Ab at room temperature for 1 h. Both the primary Ab and secondary Ab were diluted in 1% BSA and 0.3% Triton-X 100. After washing the cells, the membranes were coverslipped and mounted in ProLong Gold Antifade Reagent with 4, 6-diamidino-2-phenylindole (DAPI) (Invitrogen) to detect nuclei. Images were captured using fluorescence microscopy (FSX-100; Olympus, Tokyo, Japan).

TUNEL (TdT-Mediated dUTP Nick End Labeling) Staining

HUVECs cultured on 24-well inserts membranes described above were treated with TNF-α or staurosporine (STS) 0.5 μmol/l for 12 h. STS is an inhibitor of protein kinase C, and induces apoptosis, so is used as a positive control of apoptosis. TUNEL staining was performed using a Click-iT TUNEL Alexa Fluor Imaging Assay kit according to the manufacturer's instructions (cat. no. C10246; Invitrogen). Images were captured using fluorescence microscopy (FSX-100; Olympus, Tokyo, Japan).

Statistical Analysis

Data are reported as means ± SE. Differences in mean values were analyzed using one-way ANOVA, and Tukey's HSD test was performed as post hoc analysis (IBM SPSS statistics 23 software, Chicago, IL). Differences were considered significant with $P < 0.05$.

RESULTS

The Decrease in TER and Time of TER Recovery Were Dependent on TNF-α Concentration

Sequential TER was measured using cellZscope to evaluate the dynamic change of permeability in the TNF-α-treated HUVECs across 3 d (**Figure 1a**). When the initial stabilization of TER values (baseline) was obtained, HUVECs monolayers were treated with serially diluted TNF-α; control (0 pg/ml), 100 pg/ml, 500 pg/ml, and 2,500 pg/ml. Subsequently, the TER values decreased at all concentrations of TNF-α, and reached minimum values after between 12 and 24 h (**Figure 1b**). After reaching minimum values, the TER values of HUVECs treated with low TNF-α concentrations (100 and 500 pg/ml) recovered and increased beyond the control TER level. However, the TER values of HUVECs treated with the highest concentration of TNF-α (2,500 pg/ml) did not recover.

The decrease in TER level from baseline after TNF-α treatment and the duration required to recover the TER level to baseline were both dependent on TNF-α concentration.

The Increase in Permeability Was Also Dependent on TNF-α Concentration

A permeability assay using 70 kDa FITC-conjugated and 66–74 kDa non-FITC-conjugated dextran was performed at specific time points after TNF-α treatment to evaluate the solute permeability of HUVECs over time. Although a TNF-α concentration-dependent increase in the permeability of FITC-conjugated dextran at 12 h after TNF-α treatment was observed, the permeability of each TNF-α concentration returned to the control level at 82 h (**Figure 2**). These findings demonstrated that solute permeability was also temporarily increased in a dose-dependent manner for the period during which TER values were low, and then recovered when the TER values returned to baseline. The results of the permeability assay showed a similar pattern to TER measurement.

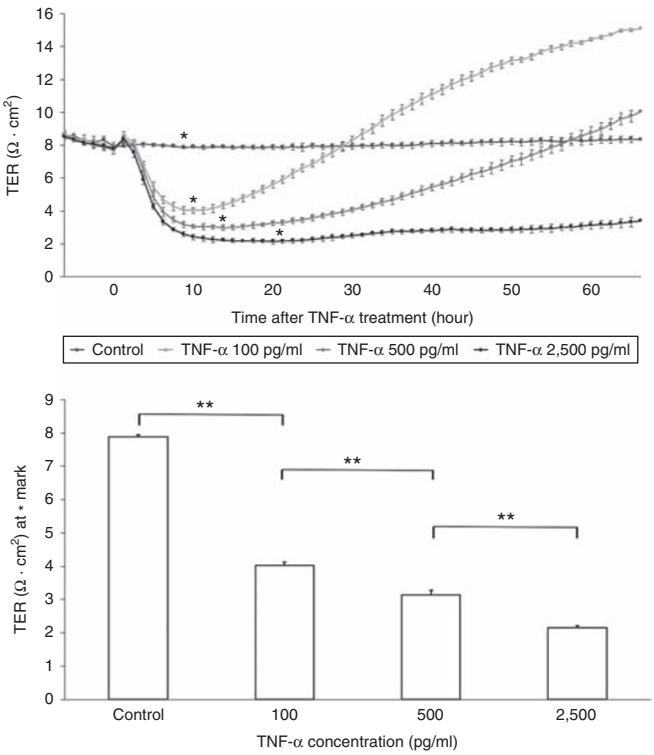

Figure 1. Dynamic change of transendothelial electrical resistance (TER) after TNF-α treatment. (**a**, upper panel) Each line shows mean TER values ($n = 4$) of each TNF-α concentration (control, TNF-α 100, 500, and 2,500 pg/ml), and error bars indicate SE. The graph is representative of three dependent experiments. (**b**, lower panel) Bars show mean minimum TER values indicated by "*" in the upper graph. Differences in mean values were analyzed using one-way ANOVA, and Tukey's honestly significant difference test was performed as *post hoc* analysis. (**$P < 0.05$).

Delocalization of Claudin-5 Was Observed After TNF-α Treatment in a Dose-Dependent Manner

Immunofluorescence staining of claudin-5, which is associated with vascular permeability, was performed using the insert membranes that were used in TER measurement and the permeability assay. Delocalization of claudin-5 and morphological spindle-shaped changes at 12 h after TNF-α treatment were observed, and the degree of claudin-5 delocalization was dependent on TNF-α concentration (**Figure 3a**). Furthermore, temporarily delocalized claudin-5 and morphological changes in HUVECs were observed at 12 h after treatment with 100 pg/ml, and each change recovered at 24 h. At 24 h, the fluorescence intensity of claudin-5 in the intracellular junction was stronger than that of the control (**Figure 3b**). These findings were consistent with the TER measurement and permeability assay results.

On the other hand, regarding nuclei stained by DAPI, few aggregated nuclei representing apoptosis were observed at all TNF-α concentrations.

High Levels of TNF-α Concentration-Induced Apoptosis in HUVECs

To investigate whether apoptosis is related to TNF-α-induced hyperpermeability in HUVECs, immunofluorescence staining

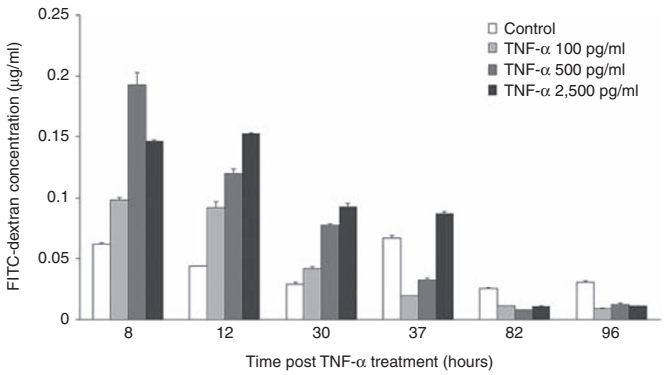

Figure 2. Results of permeability assay. A vertical axis indicates fluorescein isothiocyanate (FITC)-conjugated dextran concentration (μg/ml). A horizontal axis shows the time after TNF-α treatment. Fluorescence intensity of FITC-conjugated dextran leaking from the upper to the lower chambers of Transwell membranes was measured in each lower chamber at specific time points after TNF-α treatment. Each bar indicates the mean FITC-conjugated dextran concentration (μg/ml) in the lower chamber ($n = 2$). White, light gray, deep gray, and black bars indicate control, TNF-α 100 pg/ ml, 500 pg/ml, and 2,500 pg/ml, respectively. Error bars indicate SE. This figure is representative of three independent experiments.

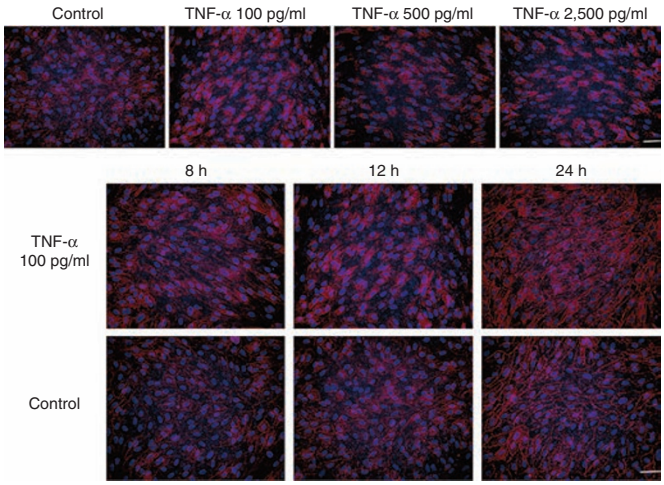

Figure 3. Immunofluorescent staining of claudin-5 in human umbilical vein endothelial cells (HUVECs) after TNF-α treatment. HUVECs-cultured on Transwell membranes were stained for claudin-5, and nuclei were counterstained with 4, 6-diamidino-2-phenylindole (DAPI) (blue) after TNF-α or control treatment at specific time points. Expression of claudin-5 (red) in HUVECs shows continuous cell membrane staining at the cell-cell borders. (**a**, upper panel) Localization of claudin-5 at 12 h after TNF-α treatment disappeared in a dose-dependent manner. Scale bar indicates 40 μm. (**b**, lower panel) Fluorescence signals of claudin-5 at the cell-cell borders delocalized transiently at 12 h after TNF-α 100 pg/ml treatment. Thereafter, localization of claudin-5 recovered at 24 h. Scale bar indicates 50 μm.

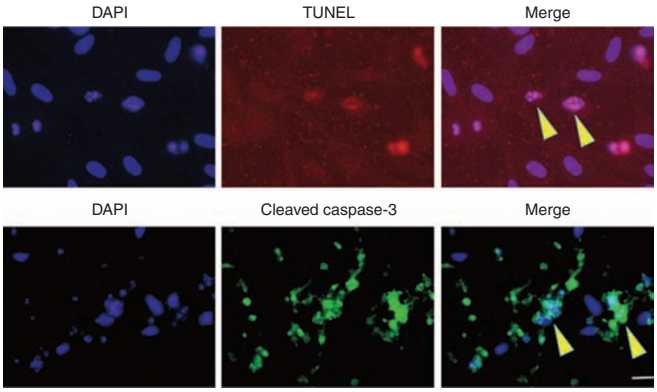

Figure 4. Typical findings of apoptotic cells in human umbilical vein endothelial cells. After TNF-α or STS treatment, apoptotic cells were observed by immunofluorescent staining for cleaved caspase-3 or TUNEL. Representative and typical apoptotic cells were shown. (**a**, upper panel) Aggregation of nuclei (blue, 4, 6-diamidino-2-phenylindole (DAPI) staining) with TUNEL (red) in the nuclei were observed. Left: DAPI staining, center; immunofluorescent staining for TUNEL; right: merged with left and central pictures. Arrowheads indicate apoptotic cells. (**b**, lower panel) Aggregation of nuclei (blue, DAPI staining) with cleaved caspase-3 (green) were observed. Left: DAPI staining, center; immunofluorescent staining for cleaved caspase-3, right; merged with left and central pictures. Arrowheads indicate apoptotic cells. Scale bar indicates 20 μm.

for cleaved caspase-3 and TUNEL were performed at 12 h post-TNF-α and STS treatment (**Figure 4** and **Figure 5a**,**b**). At the higher concentrations of TNF-α, 10 and 100 ng/ml, a few apoptotic HUVECs that were positive with cleaved caspase-3 and TUNEL were observed, but not at the lower TNF-α concentrations, 0.1 and 1 ng/ml, in both cleaved caspase-3 and TUNEL stain. To induce apoptosis in HUVECs, more than 10 ng/ml of TNF-α was required.

DISCUSSION

This study demonstrated a dynamic change of vascular permeability induced by TNF-α using TER measurement and a permeability assay. These findings well explain the disease severity and the clinical course of VAE presenting with hypercytokinemia and hyperpermeability.

Vascular hyperpermeability by disrupting the blood brain barrier and resulting brain edema could be associated with the pathophysiology of VAE (1). It was reported that the serum levels of both inflammatory cytokines and E-selectin, which induce endothelial cell damage and indicate activated endothelial cells, respectively, were high in VAE. Therefore, vascular endothelial cells would be injured in VAE (3–5).

Vascular permeability is restricted by tight junctions, which seal endothelial cells tightly. Immunofluorescence staining in the present study showed that claudin-5 was delocalized after TNF-α treatment in a dose-dependent manner, and redistribution of claudin-5 to the cell border was observed in a time-dependent manner. TER measurement also showed that a low TNF-α concentration could lead to TER recovery after an initial decrease, whereas a high TNF-α concentration (2,500 pg/ml) could not. In severe encephalopathy cases with poor prognosis, serum levels of inflammatory cytokines (TNF-α, IL-6, and IL-1β) were higher than those in mild cases (3–5). Our results indicate that vascular dysfunction could not be recovered in the most serious VAE cases with extremely high concentrations of inflammatory cytokines.

TNF-α is a pleiotropic cytokine produced predominantly by activated macrophages and monocytes that contribute to immune responses and inflammation. Two of the major effects of TNF-α are inducing the apoptosis signal by activating the caspase signal cascade (21), and conversely inducing the anti-apoptosis signal by stimulating nuclear factor-κB (NFκB) (22). Furthermore, TNF-α induces tight junction protein delocalization, resulting in endothelial cell hyperpermeability (23). The mechanisms of tight junction regulation by TNF-α are not fully unknown. NFκB plays a central role in TNF-α-induced hyperpermeability (24). NFκB activated by TNF-α mediates the downregulation of claudin-5 in brain endothelial cells by which the NFκB subunit p65 inactivates claudin-5 promoter activity, resulting in a decrease in claudin-5 expression and increase in vascular permeability (25). Another mechanism of tight junction regulation is endocytosis of the tight junction protein. The endocytosis of transmembrane proteins is important in the regulation of tight junction and vascular permeability, which plays a role in TNF-α-induced tight junction disruption (26). NFκB can also increase the expression of myosin light chain kinase (MLCK) in TNF-α-induced hyperpermeability. MLCK is a kinase of myosin light chain (MLC), which is a cytoskeletal protein and connects to the tight junction protein. The phosphorylation of MLC can induce caveolae-mediated endocytosis of the tight junction protein (27).

On the other hand, in severe VAE with bad prognosis, the values of serum cytochrome c, which is associated with

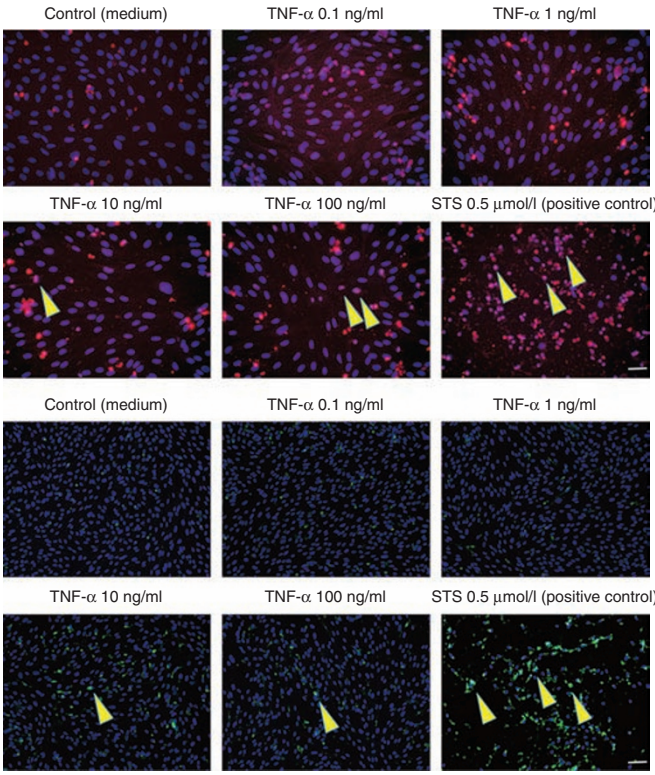

Figure 5. Apoptosis in human umbilical vein endothelial cells (HUVECs) after TNF-α treatment. Apoptotic HUVECs were detected by immunofluorescent staining for TUNEL or cleaved caspase-3 at 12 h after serially diluted TNF-α (negative control, 0.1, 1, 10, 100 ng/ml) or STS (0.5 μmol/l as positive control) treatment. Nuclei were counterstained with 4, 6-diamidino-2-phenylindole (DAPI) (blue). (**a**, upper panel) Arrowheads indicate TUNEL-positive cells as seen in Figure 4. At positive control and higher TNF-α (10, 100 ng/ml), apoptotic cells were detected, but not at negative control and lower TNF-α (0.1, 1 ng/ml). Scale bar indicates 40 μm. (**b**, lower panel) Arrowheads indicate cleaved caspase-3-positive cells as seen in figure 4. At positive control and higher TNF-α (10, 100 ng/ml), apoptotic cells were detected, but not at negative control and lower TNF-α (0.1, 1 ng/ml). Scale bar indicates 80 μm.

apoptosis, were higher than those in mild cases. Furthermore, neurons and glial cells undergoing apoptosis were observed in a histological section of necropsy in VAE patients, so it seems that apoptosis is related to the pathophysiology of VAE (1,28–30). The results of immunofluorescent staining in the present study showed that apoptotic cells were not observed under the condition of less than 1 ng/ml of TNF-α, but were observed under extremely high levels of TNF-α, 10 ng/ml, and 100 ng/ml. It has been previously reported that the apoptosis-inducing TNF-α concentration was approximately 20–100 ng/ml (31–33). In VAE patients with bad prognosis, the clinically observed serum TNF-α values were 75.7 ± 65.8 pg/ml (5). These values were in the picogram range, and were much lower than apoptosis-inducible TNF-α values *in vitro*. Local TNF-α concentrations in the damaged endothelial cells might be much higher than those in blood stream. T1/2 of TNF-α in plasma is also very short (6–7 min) (34). Goldblum *et al.* demonstrated that TNF-α augmented the transendothelial albumin flux in the absence of significantly increased endothelial cell cytotoxicity (35). In addition, Yilmaz *et al.* showed that high doses of TNF-α and IFN-γ induced reversible alterations in the cell morphology without a significant increase in the rate of apoptosis (36). Hyperpermeability caused by 100 and 1,000 pg/ml of TNF-α used in this study would not be related to apoptosis but disruption of tight junction *in vitro*. On the other hand, hyperpermeability caused by extremely high TNF-α would be related to apoptosis. Therefore, vascular hyperpermeability due to vascular endothelial cell injury including apoptosis and disruption of tight junction could have key roles in the pathophysiology of severe VAE with hypercytokinemia.

In the present study, TNF-α dose-dependent dynamic TER changes of HUVECs over a period of 3 d could be analyzed in detail by using cellZscope automatically. In previous reports, an epithelial voltohmmeter (EVOM, World Precision Instruments, West Haven, CT), which measures TER using a pair of hand-held Ag/AgC1 electrodes connected to a portable voltohmmeter tool, was used to measure the TER of epithelial and endothelial cells (18,19,37). Because this method sometimes has relatively large measurement errors caused by hand-held measurements and temperature changes at every measurement procedure, it has been difficult to evaluate low TER values of vascular endothelial cells. However, impedance spectroscopy (cellZscope) used in the present study, is a new device for measuring the transendothelial impedance of cell layers under physiological conditions, and allows automated long-term monitoring of barrier-relevant parameters, including the dynamic processes within the tight junction network (18,19,38,39).

The results from TER measurement and permeability assay on the HUVECs with 2,500 pg/ml of TNF-α showed different trends from those with other concentrations. The TER level did not recover to the baseline level, but the permeability of FITC-dextran was able to recover to the control level in the HUVECs with TNF-α 2,500 pg/ml. This difference is assumed to be due to the difference in size of target molecules. Ions, the targets of TER measurement, are much smaller than 70 kDa dextran, the targets of the permeability assay.

There are some limitations to the present study. First, the cells used were not brain-derived. Expression of the tight junction protein in HUVECs differs between brain- and other organ-derived cells. Eigenmann *et al.* reported TER values of several cell lines derived from the brain vascular using cellZscope (18). The TER values shown in their study were similar to those of the HUVECs we analyzed in the present study. Second, in the present study, only TNF-α was used as a reagent to induce hyperpermeability in HUVECs. However, cytokines other than TNF-α (i.e., IL-6, IL-1β) and various factors also would affect the vascular permeability and associate with the pathophysiology of severe VAE cases. Third, the blood–brain barrier is composed of not only vascular endothelial cells, but also astrocytes, pericytes, and other tissues which constitute the neurovascular unit and interact with each other (40). However, the results of our investigation showed one aspect of the pathologies focusing on vascular hyperpermeability induced by TNF-α in VAE.

In summary and conclusion, TER measurement combined with a permeability assay is useful for evaluating vascular endothelial cell permeability in VAE in an *in vitro* model. These

evaluation methods will contribute to the development of specific treatments focusing on vascular permeability, as well as the search for novel therapeutic strategies in VAE treatment.

ACKNOWLEDGMENTS

The authors would like to thank the lab technical staff Ken Honzumi, Toshiko Sato, and Mieko Tanji for their excellent technical skills, as well as the neonatologists and obstetricians of Fukushima Medical University for the obtaining of umbilical cords. The authors are also very grateful to the mothers who donated their umbilical cords.

STATEMENT OF FINANCIAL SUPPORT

This work was supported by Grant-in-Aid for Scientific Research (C) (MEXT KAKENHI Grant Number 24591581).

Disclosure: Authors have no conflicts of interest that should be disclosed.

REFERENCES

1. Mizuguchi M, Yamanouchi H, Ichiyama T, Shiomi M. Acute encephalopathy associated with influenza and other viral infections. Acta Neurol Scand Suppl 2007;186:45–56.
2. Goenka A, Michael BD, Ledger E, et al. Neurological manifestations of influenza infection in children and adults: results of a National British Surveillance Study. Clin Infect Dis 2014;58:775–84.
3. Ichiyama T, Nishikawa M, Yoshitomi T, Hayashi T, Furukawa S. Tumor necrosis factor-alpha, interleukin-1 beta, and interleukin-6 in cerebrospinal fluid from children with prolonged febrile seizures. Comparison with acute encephalitis/encephalopathy. Neurology 1998;50:407–11.
4. Ichiyama T, Isumi H, Ozawa H, Matsubara T, Morishima T, Furukawa S. Cerebrospinal fluid and serum levels of cytokines and soluble tumor necrosis factor receptor in influenza virus-associated encephalopathy. Scand J Infect Dis 2003;35:59–61.
5. Morita H, Hosoya M, Kato A, Kawasaki Y, Suzuki H. Laboratory characteristics of acute encephalopathy with multiple organ dysfunctions. Brain Dev 2005;27:477–82.
6. Togashi T, Matsuzono Y, Takeyoshi Y, Nagano N. Pathological findings of two patients with influenza-associated encephalopathy who died with a rapid fulminant course. 2002; J Jpn Pediatr Soc 106:76–80.
7. Hoshino A, Saitoh M, Oka A, et al. Epidemiology of acute encephalopathy in Japan, with emphasis on the association of viruses and syndromes. Brain Dev 2012;34:337–43.
8. Kasai T, Togashi T, Morishima T. Encephalopathy associated with influenza epidemics. Lancet 2000;355:1558–9.
9. Hu YJ, Wang YD, Tan FQ, Yang WX. Regulation of paracellular permeability: factors and mechanisms. Mol Biol Rep 2013;40:6123–42.
10. Capaldo CT, Nusrat A. Cytokine regulation of tight junctions. Biochim Biophys Acta 2009;1788:864–71.
11. Chiba H, Osanai M, Murata M, Kojima T, Sawada N. Transmembrane proteins of tight junctions. Biochim Biophys Acta 2008;1778:588–600.
12. Morita K, Furuse M, Fujimoto K, Tsukita S. Claudin multigene family encoding four-transmembrane domain protein components of tight junction strands. Proc Natl Acad Sci USA 1999;96:511–6.
13. Morita K, Sasaki H, Furuse M, Tsukita S. Endothelial claudin: claudin-5/TMVCF constitutes tight junction strands in endothelial cells. J Cell Biol 1999;147:185–94.
14. Nitta T, Hata M, Gotoh S, et al. Size-selective loosening of the blood-brain barrier in claudin-5-deficient mice. J Cell Biol 2003;161:653–60.
15. Bressler J, Clark K, O'Driscoll C. Assessing blood-brain barrier function using *in vitro* assays. Methods Mol Biol 2013;1066:67–79.
16. Karasaki Y. [Isolation of endothelial cells from human umbilical cords and development of low-cost culture medium]. J UOEH 1996;18:281–5.
17. Jaffe EA, Nachman RL, Becker CG, Minick CR. Culture of human endothelial cells derived from umbilical veins. Identification by morphologic and immunologic criteria. J Clin Invest 1973;52:2745–56.
18. Eigenmann DE, Xue G, Kim KS, Moses AV, Hamburger M, Oufir M. Comparative study of four immortalized human brain capillary endothelial cell lines, hCMEC/D3, hBMEC, TY10, and BB19, and optimization of culture conditions, for an *in vitro* blood-brain barrier model for drug permeability studies. Fluids Barriers CNS 2013;10:33.
19. Horiuchi T, Matsunaga K, Banno M, et al. HPMCs induce greater intercellular delocalization of tight junction-associated proteins due to a higher susceptibility to H2O2 compared with HUVECs. Perit Dial Int 2009;29:217–26.
20. Beese M, Wyss K, Haubitz M, Kirsch T. Effect of cAMP derivates on assembly and maintenance of tight junctions in human umbilical vein endothelial cells. BMC Cell Biol 2010;11:68.
21. Robaye B, Mosselmans R, Fiers W, Dumont JE, Galand P. Tumor necrosis factor induces apoptosis (programmed cell death) in normal endothelial cells *in vitro*. Am J Pathol 1991;138:447–53.
22. Fan Y, Dutta J, Gupta N, Fan G, Gélinas C. Regulation of programmed cell death by NF-kappaB and its role in tumorigenesis and therapy. Adv Exp Med Biol 2008;615:223–50.
23. McKenzie JA, Ridley AJ. Roles of Rho/ROCK and MLCK in TNF-alpha-induced changes in endothelial morphology and permeability. J Cell Physiol 2007;213:221–8.
24. Ma TY, Iwamoto GK, Hoa NT, et al. TNF-alpha-induced increase in intestinal epithelial tight junction permeability requires NF-kappa B activation. Am J Physiol Gastrointest Liver Physiol 2004;286:G367–76.
25. Aslam M, Ahmad N, Srivastava R, Hemmer B. TNF-alpha induced NFκB signaling and p65 (RelA) overexpression repress Cldn5 promoter in mouse brain endothelial cells. Cytokine 2012;57:269–75.
26. Utech M, Mennigen R, Bruewer M. Endocytosis and recycling of tight junction proteins in inflammation. J Biomed Biotechnol 2010;2010:484987.
27. Stamatovic SM, Keep RF, Wang MM, Jankovic I, Andjelkovic AV. Caveolae-mediated internalization of occludin and claudin-5 during CCL2-induced tight junction remodeling in brain endothelial cells. J Biol Chem 2009;284:19053–66.
28. Hosoya M, Kawasaki Y, Katayose M, et al. Prognostic predictive values of serum cytochrome c, cytokines, and other laboratory measurements in acute encephalopathy with multiple organ failure. Arch Dis Child 2006;91:469–72.
29. Nunoi H, Mercado MR, Mizukami T, et al. Apoptosis under hypercytokinemia is a possible pathogenesis in influenza-associated encephalopathy. Pediatr Int 2005;47:175–9.
30. Hosoya M, Nunoi H, Aoyama M, Kawasaki Y, Suzuki H. Cytochrome c and tumor necrosis factor-alpha values in serum and cerebrospinal fluid of patients with influenza-associated encephalopathy. Pediatr Infect Dis J 2005;24:467–70.
31. Sumikoshi M, Hashimoto K, Kawasaki Y, et al. Human influenza virus infection and apoptosis induction in human vascular endothelial cells. J Med Virol 2008;80:1072–8.
32. Koshio O, Nagao T, Mabuchi A, Ono Y, Suzuki K. Apoptotic signaling in endothelial cells with neutrophil activation. Mol Cell Biochem 2012;363:269–80.
33. Mi J, Zhang X, Liu Y, et al. NF-kappaB inhibition by an adenovirus expressed aptamer sensitizes TNFalpha-induced apoptosis. Biochem Biophys Res Commun 2007;359:475–80.
34. Beutler BA, Milsark IW, Cerami A. Cachectin/tumor necrosis factor: production, distribution, and metabolic fate in vivo. J Immunol 1985;135:3972–7.
35. Goldblum SE, Hennig B, Jay M, Yoneda K, McClain CJ. Tumor necrosis factor alpha-induced pulmonary vascular endothelial injury. Infect Immun 1989;57:1218–26.
36. Yilmaz A, Bieler G, Spertini O, Lejeune FJ, Rüegg C. Pulse treatment of human vascular endothelial cells with high doses of tumor necrosis factor and interferon-gamma results in simultaneous synergistic and reversible effects on proliferation and morphology. Int J Cancer 1998;77:592–9.
37. Honda M, Nakagawa S, Hayashi K, et al. Adrenomedullin improves the blood-brain barrier function through the expression of claudin-5. Cell Mol Neurobiol 2006;26:109–18.
38. Hemmersbach S, Brauer SS, Hüwel S, Galla HJ, Humpf HU. Transepithelial permeability studies of flavan-3-ol-C-glucosides and procyanidin dimers and trimers across the Caco-2 cell monolayer. J Agric Food Chem 2013;61:7932–40.
39. Benson K, Cramer S, Galla HJ. Impedance-based cell monitoring: barrier properties and beyond. Fluids Barriers CNS 2013;10:5.
40. Dalkara T, Gursoy-Ozdemir Y, Yemisci M. Brain microvascular pericytes in health and disease. Acta Neuropathol 2011;122:1–9.